Posterior Distribution for the Pulse Width Modulation of a Square Wave Conditional on Digital Measurements of its On-Off Components

by

Frank Lad

Department of Mathematics and Statistics

University of Canterbury, Christchurch, New Zealand

and

G.R. Dunlop

Department of Mechanical Engineering

University of Canterbury, Christchurch, New Zealand

No. 134 January, 1996

Abstract – We derive an exact formulation of the posterior density and distribution of the pulse width modulation of a square wave, produced by an electronic sensor monitored by digital counts of a vibrating crystal. The density is a differentiable rational function, with nodes at which its second derivative is discontinuous. As a result, the distribution function mimics a "constant jolt" system. The posterior is based upon prior assertions that exemplify the theory of precise measurement. The analysis provides an extremely complicated application of elementary arguments in the theory of multiple integration of transformed functions over the unit-cube. All algebraic detail is generated by MAPLE programming.

Keywords – Precise Measurement, Constant Jolt System, Heaviside Function.

Posterior Distribution for the Pulse Width Modulation of a Square Wave Conditional on Digital Measurements of its On-Off Components

Frank Lad and G. R. Dunlop

Dept. of Mathematics and Statistics Dept. of Mechanical Engineering

University of Canterbury
Christchurch, New Zealand

7 January, 1996

1. Introduction

The square wave form of on-off electrical pulses has played a central role in the development of signal processing during the past half century. The content of the signal in a square wave form is encoded in the pulse width modulation (pwm) of the wave, that is, the fraction of the total wavelength in which the signal rests in the *on* state. First characterised in the work of Bennett (1941) for a problem in communication systems, and soon followed by an application in servomotor control (Kretzmer, 1947), pulse techniques are by now ubiquitous in all fields of electronic information transmission. The specific application that has motivated the research in the present article concerns an automated monitor of temperature in a solar water heater, which shall be described in detail elsewhere. Recent advances in time measurement via digital counts of a rapidly vibrating crystal allow very precise measurements of the on and off components of a wave. However, most applications still rely on a crude estimate of the pwm, computed as the number of counting vibration clicks recorded during the *on* component of a wave relative to the total clicks recorded during a complete wave signal.

In the present paper we derive for th first time an exact algebraic formulation of the posterior distribution of the pwm conditioned on digital measurements of a single wave's *on* and *off* components, in the context of prior information that is appropriate to the theory of precise measurement. In a word, this theory presumes that prior information regarding the pwm is very mild relative to the sharpness of the information contained in the precise digital measurement of the wave components. To summarise our results, the distribution function, its density, and the density's derivative are all found to be continuous rational functions. However the second derivative of the density is discontinuous at four nodes, and to a fine degree of approximation it mimics the features of a "constant jolt" system.

In Section 2 we formalise our characterisation of a square wave pulse and its notation. Section 3 continues the formalisation of the digital measurement structure for components of the wave. Knowledge of the exact state of the wave is shown to depend on three identifiable components of uncertainty. Section 4 specifies precisely the prior information that is appropriate to this measurement problem, and identifies some transformations of the uncertainty distribution that are relevant to the analysis. Section 5 presents the derivation strategy for identifying the posterior distribution and its solution. Section 6 presents the summary characteristics of its first two moments. Section 7 concludes this paper with a display of the posterior distribution function and its density, conditioned on $M_1 = 100$ and $N_1 = 1000$, and a commentary on its first three derivatives. The detailed analysis presented in this paper pertains only to the first recorded wave, but the notation structure allows an extension of our analysis to further waves, to be considered in a subsequent report.

2. Formalising a Square Wave Signal: Definitions and Notation

An electronic sensing device records a pulsating signal in the form of a *square wave* as shown in Fig. 1. The information content of the signal is specified by the pulse width modulation ratio, τ/T, defined as the *on* time duration of a pulse relative to the period of a complete pulse, and referred to throughout this paper as the pwm of the signal.

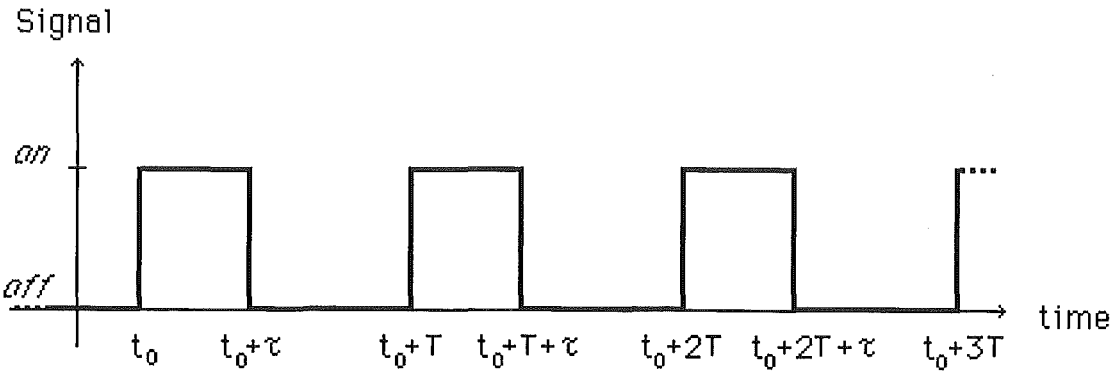

Figure 1. A square wave of pulsating signals. At a fixed pwm ratio, the sensor receives electrical pulses in a square wave form. As shown, the first pulse begins in the *on* state at time t_0, and remains in that state through time $t_0+\tau$, at which time the pulse shifts to the *off* state until time t_0+T. At this time the signal repeats, the pulse shifting to the *on* state again for a time duration of width τ, then *off* for a time of width $T-\tau$, and so on.

A statistical measurement system is designed to assess the pwm ratio of a signal, which is presumed to change very slowly with respect to the duration of one; or even several squarewave pulses, each of length T. Thus, the

sizes of τ and T can be presumed to be constant over the period of several wavelengths of the recorded signal. The goal of our statistical analysis is to derive the posterior distribution (and summary moments) of uncertain knowledge about τ/T conditioned on highly precise but inexact digital measurements of τ and T over one (and subsequently two) complete signal wave(s). An algebraic solution to this problem shall be provided in the context of the theory of precise measurement (Edwards, Lindman, and Savage, 1963, with extensions by Dickey, 1976). While a system engineer will invariably have some prior information regarding the pwm of the emitted signal wave, based on uncertain knowledge of the system being monitored, this information is typically very mild relative to the fairly precise measurements of τ and T provided by digital measurement which we shall now describe.

3. Digital Measurements of the Signal Wave Components

Measurements of the time that a signal pulse remains in the *on* state and the *off* state are made in terms of integer counts of a rapidly vibrating crystal, which repeats constantly over time intervals of extremely short known duration, denoted by Δ. The scale of Δ is typically small relative to τ, which is itself quite small. To monitor the pwm ratio over the brief time interval of a measurement, the pulse meter records sequential values of the number of clicks of the vibrating crystal occurring during the first signal *on* period, M_1, during the first complete cycle, N_1, during the second signal *on* period M_2, during the second complete cycle, N_2, and so on. Formally, we define the sequence of quantities M_i and N_i, for $i = 1,2, \ldots$, by

$M_i \equiv$ the number of crystal pulse clicks recorded during the time interval $[t_0 + (i-1)T,\ t_0 + (i-1)T + \tau)$, and

$N_i \equiv$ the number of crystal pulse clicks recorded during the time interval $[t_0 + (i-1)T,\ t_0 + iT)$.

Thus, the counts M_i identify pulse clicks recorded during the *on* state of the i^{th} signal wave, whereas the counts N_i identify the clicks recorded *throughout* the i^{th} complete wave.

Although the values of τ and T are presumed constant over an entire measurement recording interval of a few square wave lengths, the sequential measurements $M_1, M_2, M_3, \ldots$ and $N_1, N_2, N_3, \ldots$ need not be constant. There are two related reasons for this: the incommensurability of the time width of the on and off states of the signal wave with the period Δ of a counting cycle, and the phase relation of the counting cycle with the signalling wave. We shall examine each of these in turn.

3.1. Two Incommensurability Fractions: ϵ_τ and ϵ_T

Firstly, the discreteness of the crystal vibration count allows that neither the time duration of the *on* phase of the wave signal nor the duration of the complete wave need be an integer multiple of the count recording interval, Δ. We can represent this explicitly by the defining equations

$$\tau = M\Delta + \epsilon_\tau\Delta \qquad \text{and} \qquad T = N\Delta + \epsilon_T\Delta \ , \tag{1}$$

where M and N are fixed integers depending on the relative sizes of Δ, τ, and T, and ϵ_τ and ϵ_T are each fractions within the interval [0, 1). The unobservable values of ϵ_τ and ϵ_T so defined derive from the incommensurability of the width of the *on* portion of a signal wave, τ, and of the complete wave width, T, with the time width of the crystal counting cycle, Δ.

Figure 2 illustrates the sizes of ϵ_τ and ϵ_T relative to the sizes of M and N and the crystal pulse interval, Δ, *presuming that* the counting crystal has clicked at the final instant of the off state, $)t_0$, just when the signalling wave jumps from an *off* state to the *on* state. (The crystal count time line shown at the top of Fig. 2 designates this click as count number "0", since it occurs when the signal pulse is still in the *off* state, prior to the first recorded click in the *on* state.) In this scenario, the initial counting cycle is perfectly in phase with the beginning of the first signal wave in the on state, so the first click of the crystal is recorded at time $t_0 + \Delta$. We shall modify this supposition shortly.

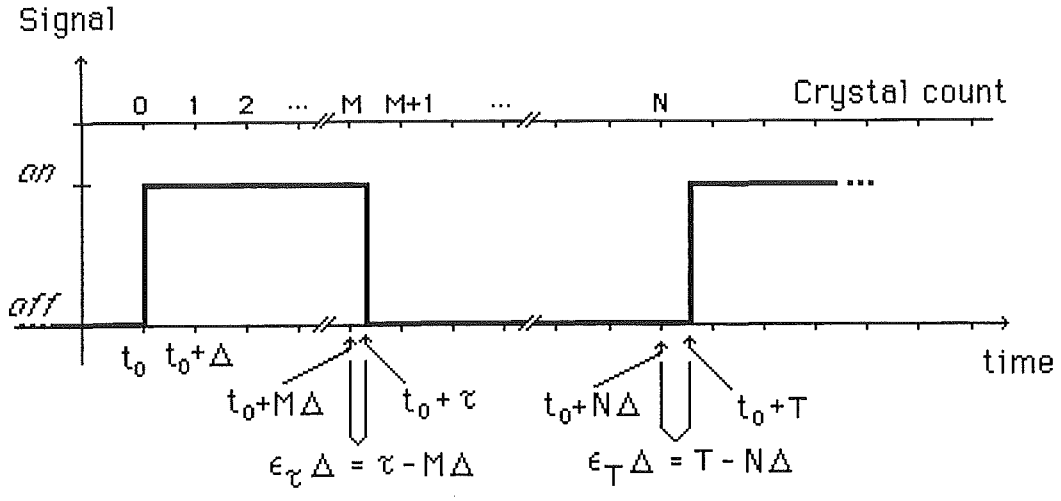

Figure 2. A square wave with (on, on+off) time widths of (τ, T) determines the values of M and ϵ_τ, along with N and ϵ_T, in terms of the counting crystal pulse time width, Δ. In this example, the crystal vibration time-counting interval is designated as beginning at time t_0, precisely in phase with the jump in the signalling wave from the *off* to the *on* state. So the first "count" is registered precisely at time $t_0 + \Delta$. As shown in this illustration, the size of ϵ_τ is less than ϵ_T, but this need not be so.

3.2. The Phase Relation of the Signal Pulse to the Counting-Cycle: ϵ_0

A second factor in understanding the relation of recorded counts M_i and N_i to the signal pulse widths τ and T is that the first recorded click of the crystal counter does not necessarily occur precisely 1Δ time unit after the wave form has jumped from the *off* to the *on* state of the signal. All that is known when the recording in the *on* state begins, is that the previous click was recorded while the sensor was in the *off* state, and that the first recorded click occurred in the *on* state. The jump in the signalling state from off to on could have occurred anywhere in time between these two clicks, from "just after" the last off-state click at one extreme (as presumed in the illustration of Fig. 2), to "just before" the first on-state click at the other extreme. Figure 3 illustrates two such possibilities, exemplifying different numerical values for the time duration we shall denote by ϵ_0, defined as the fraction of a time interval Δ that the signalling pulse emits in the *on* state after the final click is recorded in the *off* state but before the first click is recorded in the *on* state. The value of ϵ_0 associated with the situation of Fig. 2 is $\epsilon_0 =)1$.

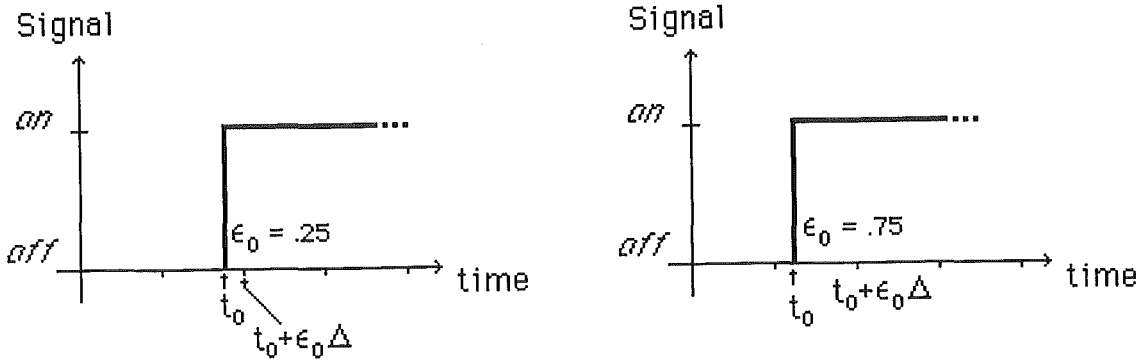

Figure 3. Two examples of possible sizes of $\epsilon_0 \in [0,1)$. In the example at left, ϵ_0 = .25, while at right ϵ_0 = .75. The value of ϵ_0 is defined as the fraction of a time interval Δ that the signalling wave emits in the *on* state after the final click recorded in the *off* state and before the first click is recorded in the *on* state, beginning the count accumulation that will specify the value of M_1.

3.3. Digital Crystal Counts as a Function of M, N, ϵ_0, ϵ_τ, and ϵ_T

Now for given values of τ and T, the observed sequence of measured crystal pulse counts $\{M_1, N_1, M_2, N_2, \ldots\}$ is the result of a specifiable function of the non-measurable values of ϵ_0, ϵ_τ, and ϵ_T. This function is specified recursively as follows. For the first square wave signal,

$$M_1 = M + 1 - (\epsilon_0 \geq \epsilon_\tau) \qquad \text{and} \qquad N_1 = N + 1 - (\epsilon_0 \geq \epsilon_T) \ , \qquad (2)$$

where parentheses around the inequalities denote the integer 1 if the inequality holds, and the number 0 if not (a variant of the Heaviside function). The pair of function values in equation (2) can be understood by examining Fig. 4 (next page).

The signalling wave being assessed is emitted in some specific form such as that depicted in Fig. 4a, though none of the values of t_0, τ, M, ϵ_τ, T, N, or ϵ_T are known. (In this illustration, the value of $\epsilon_\tau < \epsilon_T$, but this inequality could be reversed as well.) In the context of such a wave, three different pairs of measured values (M_1, N_1) could result, depending further on the size of ϵ_0. For the vibrations of the crystal counter may be in a range of possible phase relations with the square wave signal pulse. The precise phase relation is determined by the unknown value of ϵ_0. The only three possibilities in the context of $\epsilon_\tau < \epsilon_T$ are illustrated in the lines b, c, and d of Fig. 4.

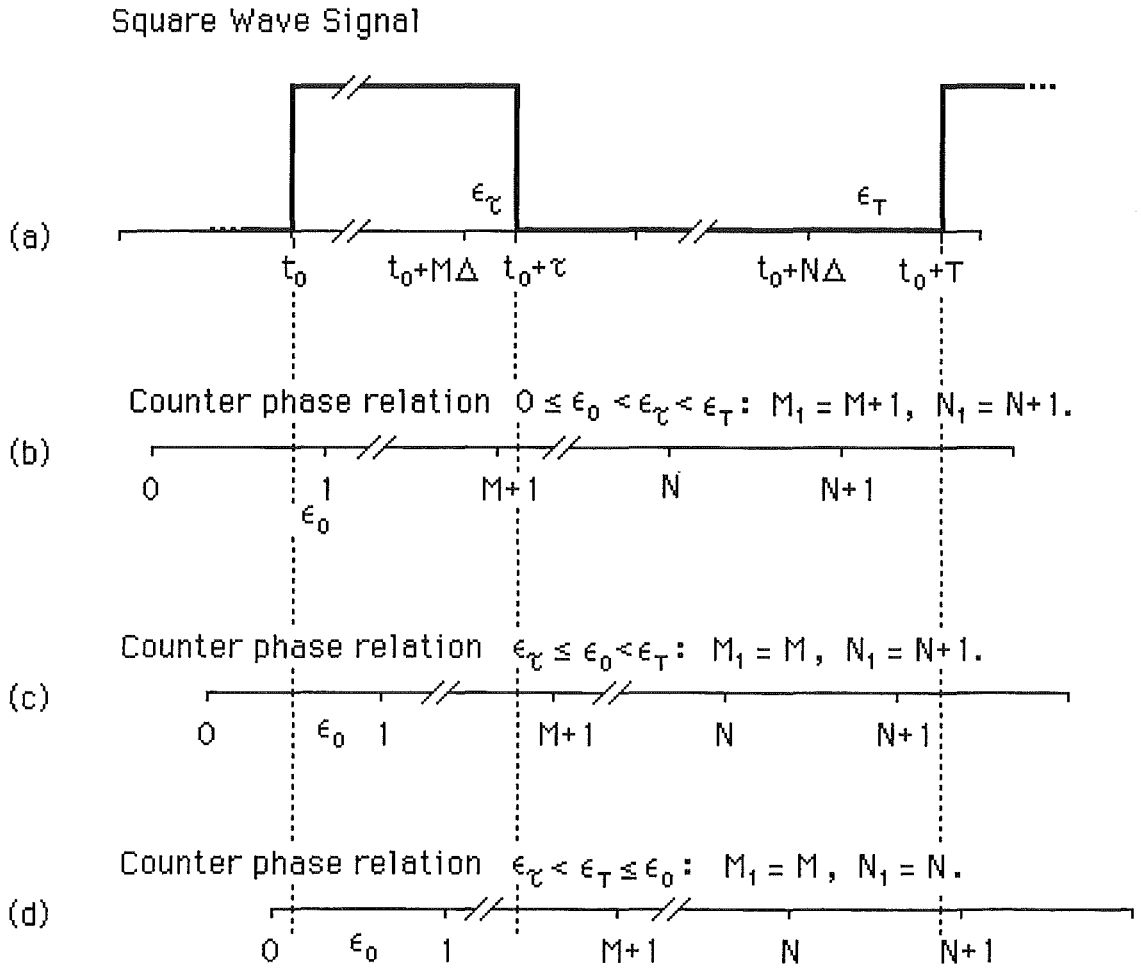

Figure 4. Three possible phase relations of the counting cycle with the square wave signal. For fixed values of M, N, and $\epsilon_\tau < \epsilon_T$, displayed in line (a) the size of ϵ_0 determines the pulse counts (M_1, N_1) as either (M+1, N+1), (M, N+1), or (M, N), as shown in lines b, c, and d, for increasingly large values of ϵ_0. If $\epsilon_\tau \ge \epsilon_T$, the corresponding comparison would show the possible counts (M_1, N_1) to be (M+1, N+1), (M+1, N), and (M, N).

In Fig. 4b, the first stroke of the counter would occur very shortly after the signal wave jumps into the *on* state, a situation resulting whenever

$0 \leq \epsilon_0 < \epsilon_\tau$. In such a case, $M_1 = M+1$ clicks of the crystal would be recorded while the signal is in the *on* state of the square wave. The first count would be registered at the time $t = t_0 + \epsilon_0$, that is, very shortly after time t_0; the count M+1 would be recorded at $t = t_0 + \epsilon_0 + M\Delta$, which is before the time $t_0 + \tau$; and the crystal count would continue with the square wave shifted into its *off* state through the count $N_1 = N+1$, registered at time $t = t_0 + \epsilon_0 + N\Delta$, that is, before the time $t_0 + T$ when the signal would shift again to the *on* state.

Only if ϵ_0 is large enough to equal or exceed ϵ_τ would the $M+1^{st}$ stroke of the counting crystal be recorded during the current-off state of the signal wave, thus determining $M_1 = M$. Such a situation is illustrated in Fig. 4c, for which the three ϵ values satisfy $\epsilon_\tau \leq \epsilon_0 < \epsilon_T$. However the size of ϵ_T is still large enough that the $N+1^{st}$ crystal click would be recorded during the *off* state of the complete square wave, before a second wave signal emission begins.

Finally, if the phase shift of the crystal counter corresponds to an even larger relative value of ϵ_0, satisfying $\epsilon_\tau < \epsilon_T \leq \epsilon_0$, as exemplified in Fig. 4d, both the $M+1^{st}$ crystal click would be recorded during the *off* state of the signal wave, and the $N+1^{st}$ click would not be recorded until the *on* state of the second square wave signal. In such a context the measured values of M_1 and N_1 would only equal M and N.

In this way, the recorded values of M_1 and N_1 are determined by the unknown relative sizes of ϵ_0, ϵ_τ, ϵ_T, τ, and T (or equivalently, of ϵ_0, ϵ_τ, ϵ_T, M and N) according to the pair of equations we have numbered (2). The three possible observation pairs for (M_1, N_1) when $\epsilon_\tau < \epsilon_T$ are (M+1, N+1), (M, N+1), and (M, N), as pictured in lines b, c, and d of Fig. 4. A similar analysis of the alternative situation when $\epsilon_\tau \geq \epsilon_T$ concludes that the possible measurement recordings of the crystal counts are $(M_1, N_1) = (M+1, N+1)$, occurring when $\epsilon_0 < \epsilon_T \leq \epsilon_\tau$, or $(M_1, N_1) = (M+1, N)$ when $\epsilon_T \leq \epsilon_0 < \epsilon_\tau$, or finally, $(M_1, N_1) = (M, N)$, occurring when $\epsilon_T \leq \epsilon_\tau \leq \epsilon_0$.

4. Uncertainty Assertions Regarding τ/T, Specified via a Conditional Distribution for the Epsilons given M_1 and N_1

Understanding now the roles of the unobserved values of ϵ_0, ϵ_τ, and ϵ_T in the identification of τ and T and of the observable sequence M_1 and N_1, under conditions of precise measurement it would be reasonable to regard the three epsilons independently and each uniform on [0, 1) conditional on the values of M_1

and N_1, no matter what integers these happen to be, but especially in the case that they are large numbers. (This would reflect the fact that the counting crystal vibrates rapidly relative to the duration of the square wave pulse.) This uniform prior assertion is motivated by three considerations: that the counting cycle and the square wave may be in any phase relation whatsoever within [0, 1); that the fractional incommensurability of the on and the off components of the square wave with the period of the crystal vibration may each be of any magnitude within [0, 1); and moreover, that the observed values of M_1 and N_1 are completely uninformative with respect to the magnitudes of the three ϵ values which identify these relations.

For the present technical report, it is worth remarking that this is a rather unusual form for expressing prior information, represented by a conditional probability distribution given the data. But it will be recognised as eminently meaningful in the context of the operational subjective tradition of probability along the lines developed by Bruno de Finetti (1974, 1975) and his followers. See Scozzafava (1991) for example, and the discussion of Hill (1986). In the analysis which follows, we shall derive the implications of this "conditionally uniform" assertion about the three epsilons for the operationally useful derivation of a the posterior distribution of the pwm, τ/T, conditional only on the measured quantities M_1 and N_1. It is also worth mentioning that the non-informative assertion about the epsilons conditional on M_1 and N_1, which formalises this assertion of "prior" information, will imply a specific form of interdependent information regarding the epsilons contained in digital measurements of a second square waveform. Details on this matter are deferred to a separate report.

Of immediate interest and relevance to our impending derivations is to notice that the conditional uniformity of the distribution asserted for $(\epsilon_0, \epsilon_\tau, \epsilon_T)$ within the unit cube $[0,1)^3$, conditioned on M_1 and N_1, does *not* imply a jointly uniform distribution on any pair of these epsilons when conditioning on useful subregions of the unit-cube. For purposes of reference in what follows, we state here the relevant information in the form of a simple lemma, couched in terms of the implications of a joint uniform distribution for X, Y, Z over the subregion of the unit-cube in which $0 \le x \le y \le z < 1$. In the derivations pursued in the next Section, the values of our three epsilons will alternate in playing the roles of X, Y, and Z in the following statement. For we shall consider the values of the pwm when the epsilons are conditioned separately within a six-fold partition of the unit-cube. Without further ado, let us merely state the following result, which is easily derived from elementary principles of distribution theory.

Lemma. If $(X,Y,Z) \sim$ Uniform $(0 \le x \le y \le z < 1)$, then the following joint density functions pertain:

$$f(x,y,z) = 6 \quad \text{for} \quad (0 \le x \le y \le z < 1), \quad \text{and} = 0 \text{ elsewhere;}$$
$$f(x,y) = 6(1-y) \quad \text{for} \quad (0 \le x \le y < 1), \quad \text{and} = 0 \text{ elsewhere;}$$
$$f(x,z) = 6(z-x) \quad \text{for} \quad (0 \le x \le z < 1), \quad \text{and} = 0 \text{ elsewhere;}$$
$$f(y,z) = 6y \quad \text{for} \quad (0 \le y \le z < 1), \quad \text{and} = 0 \text{ elsewhere.}$$

(Equalities at the domain boundaries can be eliminated with no effect.) Since we have noticed the relation of the relative sizes of the epsilons to the crystal vibration counts in the preceding Sections, this should be sufficient motivation for our concern with these joint densities. Let us turn to the details of their application.

5. The Pulse Width Modulation Function of the Observations, and its Posterior Distribution

Equations (1) and (2) imply that the pwm ratio can be represented as

$$\tau/T = \frac{M_1 - 1 + (\epsilon_0 \ge \epsilon_\tau) + \epsilon_\tau}{N_1 - 1 + (\epsilon_0 \ge \epsilon_T) + \epsilon_T} \tag{3}$$

The awkward feature of equation (3) relevant to deriving the posterior density $f(\tau/T \,|\, M_1, N_1)$ is the quantum jump occurring in the numerator and in the denominator when the size of ϵ_0 exceeds the barrier sizes of ϵ_τ and ϵ_T, respectively. Happily, difficulties induced by this feature can be surmounted by studying the posterior density conditional on six partitioning subregions of the unit cube, and then amalgamating the six conditional densities using standard coherency conditions on conditional and total probabilities.

The conditional distribution for $\tau/T \,|\, (M_1, N_1)$ can be determined from equation (3) by standard transformation methods if the domain of $(\epsilon_0, \epsilon_\tau, \epsilon_T)$ within the unit-cube, $[0,1)^3$, is partitioned into six regions:

Region 1A:	$\epsilon_0 < \epsilon_\tau < \epsilon_T$		Region 2A:	$\epsilon_0 < \epsilon_T \le \epsilon_\tau$	
1B:	$\epsilon_\tau \le \epsilon_0 < \epsilon_T$		2B:	$\epsilon_T \le \epsilon_0 < \epsilon_\tau$	
1C:	$\epsilon_\tau < \epsilon_T \le \epsilon_0$		2C:	$\epsilon_T \le \epsilon_\tau \le \epsilon_0$	

Regions 1A, 1B, and 1C all involve the relation $\epsilon_\tau < \epsilon_T$, while regions 2A, 2B, and 2C all imply $\epsilon_\tau \ge \epsilon_T$. The helpful feature of this partitioning is that within each of these regions the values of the events prescribing a possible quantum jump in the numerator and denominator of equation (3) are unequivocal for all

possible epsilon configurations within the region. For example, within region 1A, the value of τ/T reduces to $(M_1 - 1 + \epsilon_\tau)/(N_1 - 1 + \epsilon_T)$ since the values of both the events $(\epsilon_0 \geq \epsilon_\tau)$ and $(\epsilon_0 \geq \epsilon_T)$ are both necessarily equal to 0 when $\epsilon_0 < \epsilon_\tau < \epsilon_T$. A similar valuation of these two events occurs within each of the other five regions, though the numerical value of the valuation pair is different in each region.

Using this conditioning strategy, the value of τ/T is representable within each region in the generic form

$$\tau/T = (a + \epsilon_\tau)/(b + \epsilon_T) \qquad (4)$$

where the values of a and b are specified either as $M_1 - 1$ or M_1, and $N_1 - 1$ or N_1, respectively, depending on the region. What remains of the analysis is to use this equation to transform the conditional density $f(\epsilon_\tau, \epsilon_T \,|\, M_1, N_1, \text{Region R})$ into $f(\tau/T, \epsilon_T \,|\, M_1, N_1, \text{Region R})$ or $f(\tau/T, \epsilon_\tau \,|\, M_1, N_1, \text{Region R})$ within each of the six regions (whichever transformation is more favourable), and then to integrate out the nuisance variable to yield the "marginal" conditional density $f(\tau/T \,|\, M_1, N_1, \text{Region R})$ within each region. The resulting six region-conditional densities will then be averaged (with respect to equal probabities asserted for the six regions) to yield the desired posterior density $f(\tau/T \,|\, M_1, N_1)$.

We shall present the details of this derivation, conditioning on regions 1A and 2A, to exhibit the structure of the argument. While the logic is not at all difficult, even elementary, the complete detail is so involved that it will be left to MAPLE programming for final resolution. We shall report on the results once the logic of the derivation is clear.

Within Region 1A, the arguments ϵ_τ and ϵ_T of equation (4) play the role of the quantities Y and Z described in the joint distribution of (X, Y, Z) over $(0 \leq x < y < z < 1)$ in Section 4. To simplify the notation in what follows, we shall resolve the transformation problem in terms of the density f(y,z) over $(0 \leq y < z < 1)$ transformed to f(Q,z), where $Q \equiv (a+y)/(b+z)$ to mimic equation (4). The domain of the transformed density, exhibited in Fig. 5a, will be examined shortly. Since the inverse transformation from (Q,z) to (y,z) allows that $y = -a + (b+z)Q$, the Jacobian of the transformation from (y,z) to (Q,z) equals (b+z). Thus, the transformed density has the form

$$f(y,z) \rightarrow f(Q,z) = 6\,[-a + (b+z)Q]\,(b+z) \qquad \text{for } (Q,z) \in T(1A) \qquad (5)$$

over the appropriate transformed domain, T(1A), which we now address.

The right-hand side of Fig. 5a displays the domain of (Y,Z) relevant to our conditioning on region 1A as the set $\{(y,z) \,|\, (0 \leq y < z < 1)\}$. Considering the

transformation equation $Q \equiv (a+y)/(b+z)$, it is apparent that for any fixed value of z, the value of Q ranges from $a/(b+z)$ to $(a+z)/(b+z)$ as y ranges from 0 to z. The quadrant of positive (Z,Q) possibilities is shown at left, Q increasing to the left from 0.

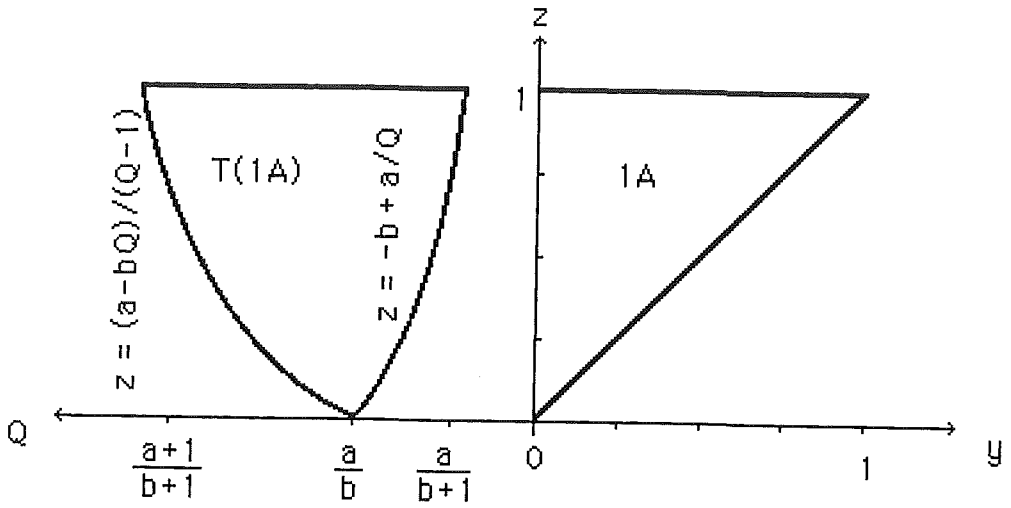

Figure 5a. The domain of (Y,Z) when conditioning on Region 1A is the upper half-unit-square at right. It is transformed to the domain T(1A) of (Q,Z) at left by the equation $Q \equiv (a+y)/(b+z)$.

Within Region 2A, the values of ϵ_Z and ϵ_T of equation (4) switch roles to those of Z and Y, respectively, in the joint distribution of (X,Y,Z) described in Section 4. In this context, the relevant transformation equation of (Y,Z) to (Q,Y) is specified as $Q \equiv (a+z)/(b+y)$. The inverse equation, $z = -a + (b+y)Q$, then identifies the Jacobian of the transformation as (b+y). Thus, the transformed density has the form

$$f(y,z) \rightarrow f(y,Q) = 6y(b+y) \quad \text{for } (y,Q) \in T(2A) \qquad (6)$$

The transformed domain, T(2A), is displayed in Fig. 5b. Considering the transformation equation $Q \equiv (a+z)/(b+y)$, it is apparent that for any fixed value of y, the value of Q ranges from $(a+y)/(b+y)$ to $(a+1)/(b+y)$ as z ranges from y to 1.

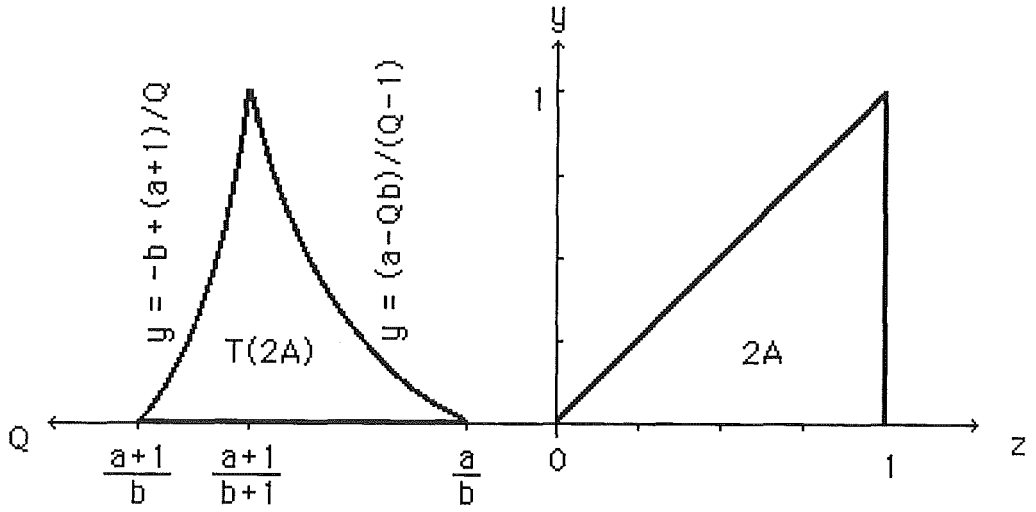

Figure 5b. The domain of (Y,Z) when conditioning on Region 2A is displayed as the lower half-unit-square at right. It is transformed to the domain T(2A) of (Q,Y) at left by the equation $Q \equiv (a+z)/(b+y)$.

The structure of the transformation analysis is identical to one of these two when conditioning restricts $(\epsilon_0, \epsilon_\tau, \epsilon_T)$ to any one of the other four regions we have specified as our partition of the unit-cube. The only differences involve changes in the roles of X, Y, and Z in representing appropriate epsilons.

The marginal density of τ/T conditional on any of the regions is achieved by integrating out the relevant nuisance variable from the transformed density, f(Q,w), where w is either x, y, or z, as appropriate to the conditioning region. The regions of integration can be understood from Figs. 5a and 5b to support the solutions

$$f(Q|1A) = \int_{-b+a/Q}^{1} 6\,[-a+(b+z)Q]\,(b+z)\,dz \quad \text{for } Q \in [a/(b+1), a/b]; \qquad (7a)$$

$$f(Q|1A) = \int_{(a-bQ)/(Q-1)}^{1} 6\,[-a+(b+z)Q]\,(b+z)\,dz \quad \text{for } Q \in [a/b, (a+1)/(b+1)]; \qquad (7b)$$

$$f(Q|2A) = \int_{0}^{(a-bQ)/(Q-1)} 6y(b+y)\,dy \quad \text{for } Q \in [a/b, (a+1)/(b+1)]; \qquad (7c)$$

$$f(Q|2A) = \int_{0}^{-b+(a+1)/Q} 6y(b+y)\,dy \quad \text{for } Q \in [(a+1)/(b+1), (a+1)/b]. \qquad (7d)$$

The limits on integration are identified by recognising in Figs. 5a and 5b that the integration is proceeding vertically with respect to z and y, respectively. Thus, the boundary functions, which are displayed in the Figures in the form of Q as a function of z (or y), must be inverted to the form of z (or y) as a function of Q, to yield the integration limits.

In every case, the result of the integration yields f(Q|Region R) in the form of a rational function of Q. For example, equation (7a) has the form $f(Q|\,1A) = c_1 Q + c_2 + c_3/Q + c_4/Q^2$ over the stated domain of Q, whereas equation (7b) has the form $f(Q|\,1A) = c_1 Q^3 + c_2 Q^2 + c_3 Q + c_4 + c_5 Q^2/(Q-1)^3$ over the stated domain.

An important feature of the integral generation of the density is that the conditional density in each region is necessarily continuous at the nodal point where the algebraic formula for the density shifts from one form to another. (In the case of region 1A, for example, this occurs when the increasing value of Q crosses the boundary of Q = a/b.) It turns out that the density is always differentiable at this nodal point as well. However, the second derivative does not exist there, since the second derivatives of the two contributing functional forms from the left and from the right are not equal. We shall observe the consequences of this jump when we examine the marginal density of τ/T aggregated over all six conditioning regions, finding that the density provides an example of a virtually "constant jolt" system.

The final detail worth mentioning is that the marginal density functions f(Q|Region R), which have been derived in light of equation (4) in terms of the parameters a and b, require a different evaluation of a and b within each of the six constituent regions partitioning the unit-cube. In both regions 1A and 2A, the values of a and b are (M1-1) and (N1-1), respectively. However, in region 1B they are M1 and (N1-1), while in region 2B they are (M1-1) and N1, and in regions 1C and 2C they are M1 and N1. The effect this has on the overall marginal density of Q (representing τ/T, remember) is that the density has a different functional form over six distinct regions of the domain. These are specified by the interval endpoints

$$\frac{(M_1-1)}{N_1} < \frac{(M_1-1)}{(N_1-1)} < \frac{M_1}{(N_1+1)} < \frac{M_1}{N_1} < \frac{M_1}{(N_1-1)} < \frac{(M_1+1)}{(N_1+1)} < \frac{(M_1+1)}{N_1} \qquad (8)$$

where these are ordered under the condition that $M_1 < (N_1-1)/2$, which implies both $(M_1+1)/(N_1+1) > (N_1-1)$ and $M_1/(N_1+1) > (M_1-1)/(N_1-1)$. The ordering is different when $M_1 = (N_1+1)/2$, and when $M_1 > (N_1+1)/2$. Within each subdomain of $f(\tau/T\,|\,M_1, N_1)$, an interval bounded by a neighboring pair in (8), a different collection of contributing component expressions designated by the partitioned

conditional densities $f(\tau/T \,|\, M_1, N_1, \text{Region R})$ is relevant to the aggregated conditional density.

The reader will appreciate by now that while none of the derivational logic is difficult, applying elementary arguments in calculus and distribution theory, the detail of its compilation is both ornate and tedious. Such conditions of a problem make it eminently appropriate for resolution using a symbolic programming language, such as MAPLE, which is the procedure we have followed. In the next two Sections we shall present characteristic details of the solution, sometimes algebraically, sometimes numerically, and sometimes graphically. We shall begin with a presentation of the exact first two moments of the conditional density for τ/T given M_1 and N_1, and proceed to an exhibition of the distribution function, the density function, and its first three derivatives. The MAPLE programs which generated the results are available from the authors.

6. Posterior Moments given a Single Measured Pulse

After all the intricacy of determining the posterior density function for the pulse width modulation based on a single measured wave, a startling feature of the result is the simplicity of its ultimate algebraic formulation. The density itself is awkward to write down, since it requires Heaviside arguments to represent its changing algebraic form over the intervals specified in line (8). Nonetheless, the first moment, or posterior mean, can be written succinctly, as

$$E[\tau/T \,|\, M_1, N_1] = 1/2 + (M_1 - N_1/2 - M_1N_1 + N_1^2/2)\log(N_1/(N_1-1)) + (M_1 - N_1/2 + M_1N_1 - N_1^2/2)\log((N_1+1)/N_1).$$

Approximating the logarithmic terms through the first three terms of their Taylor series expansion yields the approximate expression

$$E[\tau/T \,|\, M_1, N_1] \approx \frac{4M_1 - 2N_1 - 10M_1N_1 + 5N_1^2 + 14M_1N_1^2 - N_1^3 + 12M_1N_1^4 - 24M_1N_1^3}{12\,(N_1 - 1)^2\,N_1^3}$$

which is indistinguishable from M_1/N_1 for large N_1, as would be expected. The second moment (and thus the variance) of the distribution for τ/T can also be expressed exactly, but it is too long to be worth reporting. (Again, MAPLE programs that yield the exact formulas are available from the authors.)

More interesting, perhaps, are the numerical results of posterior means and variances for an array of (M_1, N_1) pairs displayed in Table 1. Notice the scale and direction of the difference between the posterior mean and M_1/N_1.

Table 1. Posterior means and variances of τ/T conditioned on M_1 and N_1. All values are exact to the number of digits displayed.

M_1	N_1	$E(\tau/T \mid M_1, N_1)$	$V(\tau/T \mid M_1, N_1)$	$SD(\tau/T \mid M_1, N_1)$
100	1000	.0999999333333066	.1516667442222779 (-6)	.3894441478 (-3)
500	1000	.5	.1250000500000307 (-6)	.3535534613 (-3)
900	1000	.9000000666666933	.1516667442222779 (-6)	.3894441478 (-3)
10	100	.0999933330666523	.1516744227799651 (-4)	.3894540060 (-2)
50	100	.5	.1250050003075619 (-4)	.3535604620 (-2)
90	100	.9000066669333476	.1516744227799651 (-4)	.3894540060 (-2)
1	10	.0993306522914530	.1524478440777893 (-2)	.3904456993 (-1)
5	10	.5	.1255030977947370 (-2)	.3542641639 (-1)
9	10	.9006693477085469	.1524478440777893 (-2)	.3904456993 (-1)

These numerical results exemplify two pleasing symmetry features of the posterior moments which can be confirmed by MAPLE, that

$$E[\tau/T \mid M_1 = m, N_1 = n] = 1 - E[\tau/T \mid M_1 = n-m, N_1 = n] \text{ , and}$$
$$V[\tau/T \mid M_1 = m, N_1 = n] = V[\tau/T \mid M_1 = n-m, N_1 = n] .$$

Together, these suggest a stronger symmetry property, also confirmed by MAPLE, that $f(\tau/T \mid M_1 = m, N_1 = n) = f(1-\tau/T \mid M_1 = n-m, N_1 = n)$. It is worth focusing in Table 1 on the very small difference between these exact posterior mean values, and the crude approximating value of M_1/N_1 in each case. Also notable, however, is how relatively large are the standard deviations of the posterior distributions, especially when the ratio of M_1 to N_1 is on the low side of .50.

Finally, it is mentionworthy for comparative purposes when results of second wave measurements are studied, that the standard deviation of τ/T given M_1 and N_1 reduces by slightly more than a factor of 10 when the sizes of M_1 and N_1 increase by a factor of 10. The scale of N_1, of course, is determined by the vibration speed of the counting crystal used to assess the values of τ and T. Since increasing speeds of crystal vibration are achieved only with increasing costs, the gain in precision achieved merits comparison with the gain achieved by continuing the signal tracking through a second wave, which is the subject of another report.

The gain in precision that is achieved by the use of our exact posterior moment formulas rather than a Monte-Carlo simulation of a τ/T generating process can be gauged by comparing Table 2 with Table 1. Table 2 presents the simulation results of generating τ/T using equation (3) based on 1 million experimental selections of $(\epsilon_0, \epsilon_\tau, \epsilon_T)$ from a uniform distribution on $[0,1)^3$, run on MATLAB. Errors in the mean, for example, amount to the order of 10^{-4} of a standard deviation when $M_1 = 100$ and $N_1 = 1000$, a reasonable scenario in many applications. The most striking content of Table 2 is how well the Monte-Carlo simulations confirm the exact derivations provided in Table 1.

Table 2. Sample averages, $\overline{X}$, sample variances, S^2, and standard deviations, S, of τ/T ratios generated from equation (3) based on 1 million experimental selections of $(\epsilon_0, \epsilon_\tau, \epsilon_T)$ from $U[0,1)^3$, using MATLAB.

M_1	N_1	$\overline{X}(\tau/T \mid M_1, N_1)$	$S^2(\tau/T \mid M_1, N_1)$	$S(\tau/T \mid M_1, N_1)$
100	1000	.10000029070	.15157 (-6)	.38931979 (-3)
500	1000	.50000071277	.12494 (-6)	.35346430 (-3)
900	1000	.89999989656	.15207 (-6)	.38996028 (-3)
10	100	.09998946195	.1515897 (-4)	.389345199 (-2)
50	100	.49999977968	.1248402 (-4)	.353327280 (-2)
90	100	.90001147993	.1514811 (-4)	.389205674 (-2)
1	10	.09931289481	.152586318 (-2)	.3906229872 (-1)
5	10	.50000554379	.125662827 (-2)	.3544895298 (-1)
9	10	.90065001568	.152530092 (-2)	.3905510109 (-1)

7. The Posterior Distribution, its Density, and Further Derivatives

We have determined in Section 5 that the posterior density function for the pwm, $f(\tau/T \mid M_1, N_1)$, is a rational function of τ/T. It is both integrable, yielding a closed form distribution function $F(\tau/T \mid M_1, N_1)$, and differentiable, yielding a rational derivative function, $f'(\tau/T \mid M_1, N_1)$. Figures 6a, 6b, and 6c display these three functions in the order of $F(\cdot)$, $f(\cdot)$, and $f'(\cdot)$ for the conditioning observation values $M_1 = 100$ and $N_1 = 1000$. While the derivative function is continuous, it is not differentiable at the nodal points identified in line (8), where the algebraic form of the density changes. Thus, the second

derivative function, $f''(\tau/T \mid M_1, N_1)$ is not continuous, but rather exhibits discontinuities at these nodal values of τ/T. This second derivative function, for these same values of M_1 and N_1, appears in Fig. 6d. The discontinuity points occur at τ/T values of

$$\frac{99}{1000} < \frac{99}{999} < \frac{100}{1001} < \frac{100}{1000} < \frac{100}{999} < \frac{101}{1001} < \frac{101}{1000} \qquad (8'')$$

which result from the evaluation of line (8) when $M_1 = 100$ and $N_1 = 1000$. The extreme left and right values in this ordering are the endpoints of the domain over which the density function is positive. In understanding the Figures, recognise that these fractions evaluate to $.099 < .0991 < .0999 < .1 < .1001 < .1009 < .101$, where rounding has been used at the fourth decimal place, unless fewer are reported.

On casual examination, Fig. 6d appears to characterise the density function as the outcome of a "constant jolt" system, in which its second derivative is constant (positive or negative) over specified jolt regions, and zero elsewhere. On closer look, you will notice that the second derivative is actually changing slightly over these intervals. Figure 6e makes this more evident by displaying the third derivative function, $f'''(\tau/T)$, which is not zero everywhere, as it would if the system were precisely the outcome of a constant jolt generator. Moreover, the second derivative of the density function, which appears in Fig. 6e to equal 0 over two large intervals of the domain, is not really equal to 0 there. It is only so small in magnitude relative to its values at the apparent jolts, that it is not visible. Figure 6f makes this clear by displaying the second derivative function values only over values of τ/T in the interval (.0991, .0999).

A final feature of the posterior density, $f(\tau/T \mid M_1 = 100, N_1 = 1000)$, worth mentioning concerns the overlap of its domain, which is [.099, .101], with the domain of the "next" conditional density, $f(\tau/T \mid M_1 = 101, N_1 = 1000)$, which is [.100, .102]. This is seen by evaluating the inequalities in line (8) for this "next" scenario of M_1 and N_1. It is pleasing that the row of ordered triangular shaped densities conforms so well to a simplistic intuition regarding the information in digital measurements about the pwm of a square wave. This feature will become much more complex, as will much more of the analysis when we examine the information in digital measurements of a following wave in the emission cycle. This will be the subject of our next report.

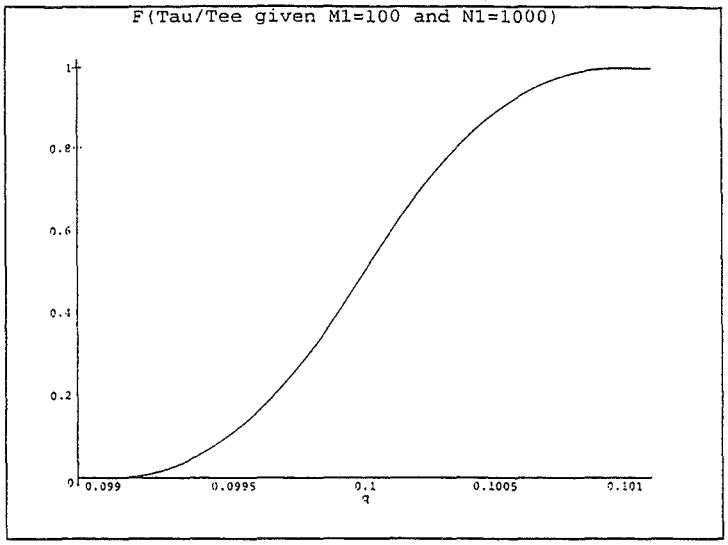

Fig 6a

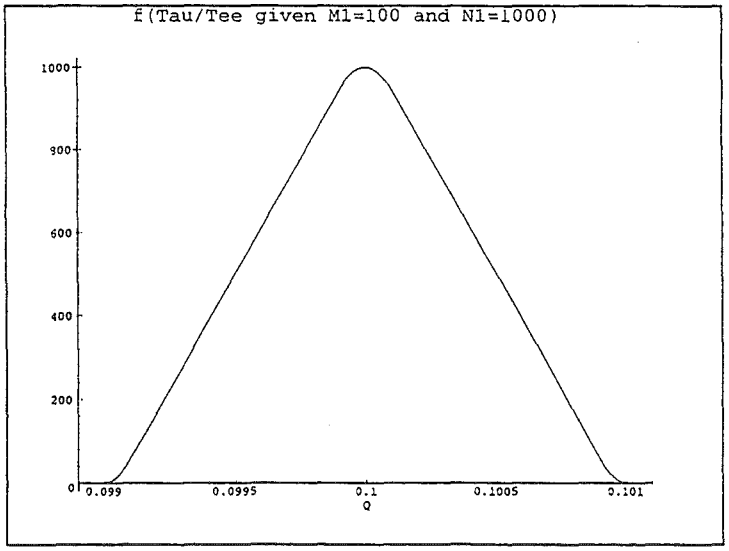

Fig 6b

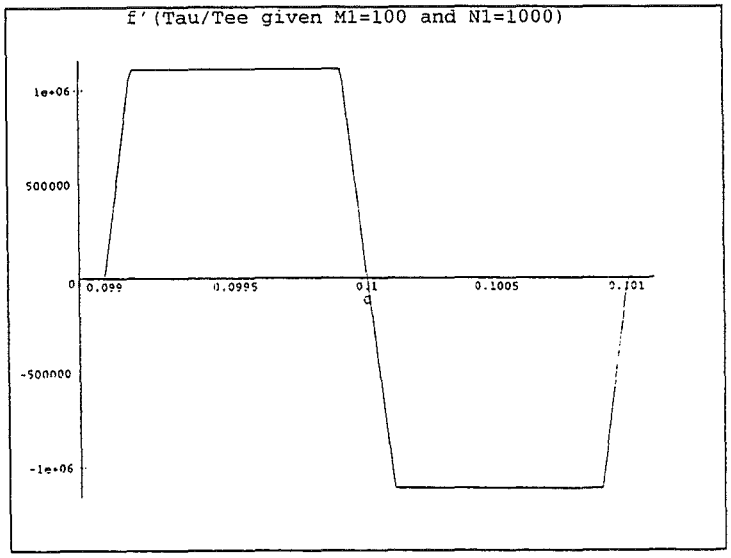

Fig 6c

Fad / Dumb

p. 17a

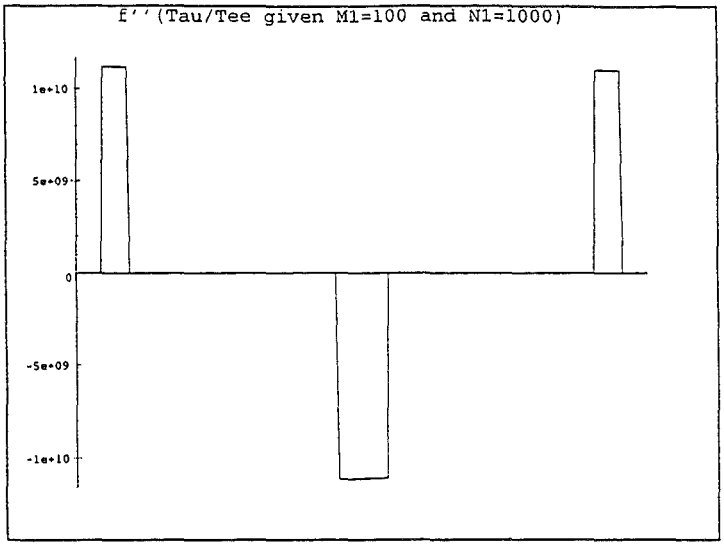

Fig 6d

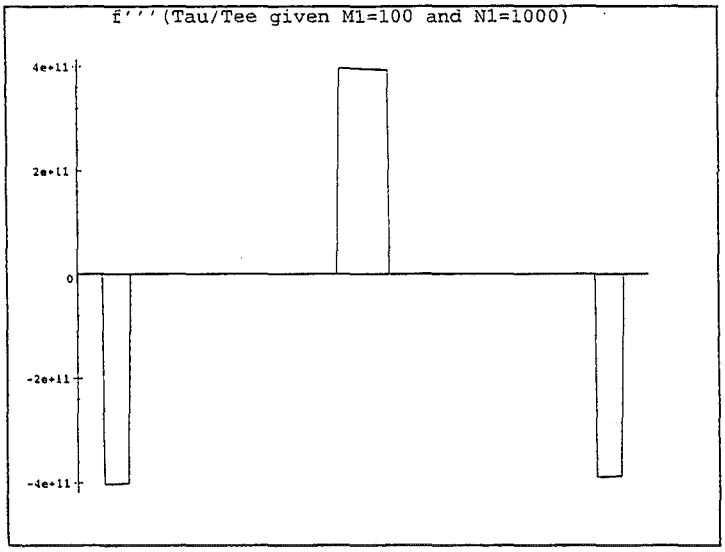

Fig 6e

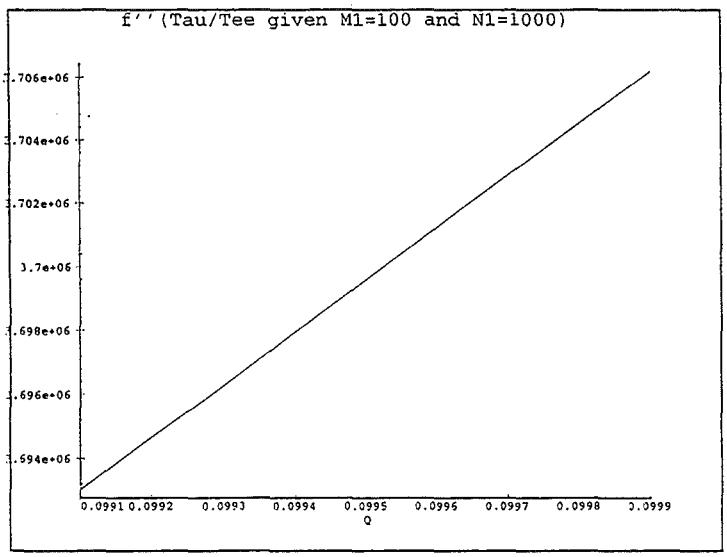

Fig 6f

Tad / Dunlop
p. 17b

References

Bennett, W. R. (1941) Time division multiplex systems, *Bell Sys. Tech. Jour.*, **20**, 191-221.

Dickey, J. M. (1976) Approximate posterior distributions, *Jour. Am. Stat. Ass.*, **71**, 680-689.

Edwards, W. A., Lindman, H. and Savage, L. J. (1963) Bayesian inference for psychological research, *Psych. Rev.*, **70**, 193-242.

de Finetti, B. (1974, 1975) *Theory of Probability*, two volumes, New York: John Wiley and Sons.

Hill, B. M. (1986) Some subjective Bayesian considerations in the selection of models, *Econometric Rev.*, **4**, 191-246.

Kretzmer, E. R. (1947) Distortion of pulse-duration modulation, *Proc. I. R. E.*, **35**, 1230-1235.

Scozzafava, R. (1991) A classical analogue of the two-slit model of quantum probability, *P. Math. App.*, Ser. C, **2**, 223-235.